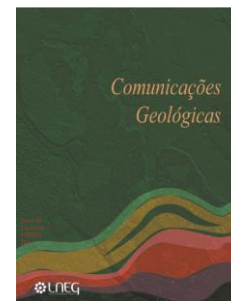


Experiments on mineral carbonation of CO₂ in gabbro from the Sines massif – first results of project InCarbon

Ensaio de carbonatação mineral de CO₂ no gabro do maciço de Sines - primeiros resultados do projeto InCarbon

P. Moita^{1,4*}, E. Berrezueta², J. Pedro^{3,4}, C. Miguel¹, M. Beltrame¹, C. Galacho^{1,5}, P. Barrulas¹, J. Mirão¹, A. Araújo^{3,4}, L. Lopes^{3,4}, J. Carneiro^{3,4}



Artigo original
Original article

Recebido em 04/11/2019 / Aceite em 16/12/2019

Publicado online em julho de 2020

© 2020 LNEG – Laboratório Nacional de Energia e Geologia IP

Abstract: The InCarbon project based on the principles of CO₂ capture and storage technologies, aims to study the potential of *in situ* mineral carbonation in mafic rocks in Alentejo. The gabbro of Sines massif was selected for the first laboratory test of mineral carbonation due to its geochemical, mineralogical and textural characteristics and proximity to the main focus of CO₂ emissions in the region. Gabbro specimens were submerged in natural brine and supercritical CO₂ for periods of 1, 4, 16 and 64 days, under 80 bar and 40 °C. The specimens were characterized before and after the experiments by means of XRD, OM, VP-SEM-EDS and ATR-FTIR, and the brine composition was analysed. Results show dissolution of silicates and textural roughness increasing with the number of days of immersion into brine. The behaviour of cations in solution after several days of testing is irregular and carbonate precipitation was not detected.

Keywords: CCS, gabbro, Sines, Brine, Supercritical CO₂.

Resumo: O projeto InCarbon, norteado pelos princípios da tecnologia de Captura e Armazenamento de CO₂, pretende estudar o potencial de carbonatação mineral *in situ* em rochas máficas do Alentejo. O gabro do maciço de Sines foi selecionado para o primeiro ensaio laboratorial de carbonatação atendendo às suas características geoquímicas, mineralógicas e texturais e à proximidade geográfica ao principal foco de emissões de CO₂ na região. Os provetes de gabro foram submersos em salmoura natural e CO₂ supercrítico durante períodos de 1, 4, 16 e 64 dias, sob 80 bar e 40 °C. Antes e após o ensaio examinaram-se os provetes com DRX, MO, VP-SEM-EDS e ATR-FTIR, e a salmoura foi analisada. Os resultados revelam dissolução dos silicatos, causando rugosidade textural que se intensifica com o tempo de imersão em salmoura. O comportamento dos catiões em solução ao fim dos vários dias de ensaio é irregular, não se detetando a precipitação de carbonatos.

Palavras-chave: CCS, gabro, Sines, Salmoura, CO₂ supercrítico.

1. Introduction

Portugal has committed to reduce significantly its greenhouse gas emissions and achieve a net balance of zero, *i.e.* carbon neutrality, by 2050 (RCN2050, 2109). Consequently, it is decisive to identify technically feasible, economically viable and socially accepted alternative paths to reduce CO₂ emissions.

One of the possible approaches is CO₂ Capture and Storage (CCS), involving CO₂ capture from large industrial or power sources and its storage in geological formations (Bachu, 2000; Benson and Cole, 2008). Adequate geological environments for CO₂ storage are provided by depleted hydrocarbon reservoirs, uneconomic coal seams, deep saline aquifers or mafic and ultramafic rock massifs (Sayegh *et al.*, 1990; Izgec *et al.*, 2008; Gaus, 2010; Saedi *et al.*, 2011; Klein and McCollom, 2013; Mateos-Redondo *et al.*, 2018).

The potential of mafic rocks for CO₂ storage rests in their ability to stabilize CO₂ via mineral carbonation (Andreani *et al.*, 2009; Klein and McCollom, 2013). The feasibility of this process was demonstrated for mafic volcanic (basalts) rocks in the CarbFix (Iceland) and Wallula (USA) projects (McGrail *et al.*, 2014; Druckenmiller and Maroto-Valer, 2005).

The FCT funded InCarbon project aims to assess the potential of using mafic and ultramafic plutonic rocks in Alentejo for storage of CO₂ captured in large stationary sources, such as those in the Sines industrial cluster. It focuses on *in situ* mineral carbonation, where CO₂ is injected into mafic rocks saturated with high salinity groundwater, promoting fast mineral carbonation and ultimately trapping the CO₂ in solid phase (carbonates).

Amongst the methodologically approaches adopted in InCarbon are CO₂-brine-rock laboratory experiments, a useful method to understand and explore the mechanisms and processes of CO₂ behaviour and interaction with the hosting rock and formation fluid (Kaszuba *et al.*, 2005; Ketzer *et al.*, 2009).

This work presents data from the first laboratory tests on the CO₂-brine-rock interaction, on a sample of gabbro from the Sines subvolcanic massif. The main goal is to assess its potential for CO₂ *in situ* carbonation. Mineralogical and textural variations of gabbro specimen and associated chemical changes in the natural brine with added supercritical CO₂, were evaluated before and after the laboratory experiments, by means of a complementary

¹Laboratório HERCULES, IIFA, Universidade de Évora, Largo Marquês de Marialva, 2, Évora, Portugal.

²Instituto Geológico y Minero de España (IGME), Oviedo, España.

³Instituto Ciências da Terra (ICT), IIFA Universidade de Évora, Rua Romão Ramalho, Évora, Portugal.

⁴Departamento de Geociências, Escola de Ciências e Tecnologia, Universidade de Évora, Portugal.

⁵Departamento de Química, Escola de Ciências e Tecnologia, Universidade de Évora, Portugal.

*Autor correspondente/Corresponding author: pmoita@uevora.pt

battery of techniques of analysis (XRD, OM, VP-SEM-EDS and ATR-FTIR).

2. Geological Setting

The Sines massif (Fig. 1) occurs on the west Portuguese coast (SW Iberia). Onshore, it has a relatively small area ($\sim 10 \text{ km}^2$), largely covered by Plio-Quaternary sediments. It exhibits an elliptical shape elongated to the offshore and interpreted by Teixeira (1962) and Ribeiro *et al.* (1979) as a sub-volcanic ring-structure. Reappraisals made on the basis of geophysical data (magnetic, gravimetric and seismic reflection) modelling suggest that the offshore section of the massif may extend along a NE–SW direction, with a total area of $\sim 300 \text{ km}^2$ (Carvalho *et al.* 1998). This massif, together with Sintra and Monchique massifs, the Volcanic Complex of Lisbon and several other minor intrusions, is part of a Late Cretaceous alkaline magmatic cycle (Ferreira and Macedo, 1979; Canilho and Abranches, 1982) to circa 22 Ma (94–72 Ma) (Miranda *et al.*, 2009).

The Sines sub-volcanic massif is mainly formed by gabbros, diorites and syenites with a profusion of dykes of variable composition (basalts, microgabbros, microdiorites, trachybasalts, lamprophyres, trachytes and microsienites; Canilho, 1972; Inverno *et al.*, 1993). Despite the Cenozoic sedimentary cover, the Geological Map of Portugal at 1/50000 scale (sheet 42-C, Santiago de Cacém, Inverno *et al.*, 1993) shows that these intrusive rocks cut the Carboniferous flysch at the South (Mira Formation) and Lower Jurassic carbonate rocks at the North. The massif is moderately fractured, and on-going characterization of the fracture patterns is fundamental for an indirect assessment of the permeability of the rock massif and, consequently, for the viability of use gabbro for in situ mineral carbonation.

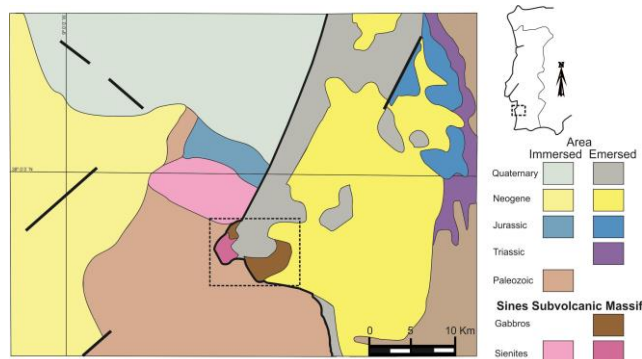


Figure 1. Location and geological setting of Sines Subvolcanic Massif. Adapted from 1/1 000 000 Geologic Mapping of Portugal (LNEG, 2010).

Figura 1. Localização e enquadramento geológico do Maciço Subvolcânico de Sines. Adaptado da Carta Geológica de Portugal a 1/1 000 000 (LNEG, 2010).

3. Methodology

A coarse-grained gabbro was sampled at a cliff near Praia do Norte (Sines) and cut in 50 test cubes with 27 cm^3 each and 4 with 1 cm^3 , afterwards divided in 4 test sets and one reference set (0-day set). The specimens – seven cubes of 27 cm^3 , two parallelepipeds of $27/2 \text{ cm}^3$ and one of 1 cm^3 – were immersed in a high salinity brine saturated in CO_2 in a hyperbaric chamber simulating CO_2 conditions in a geological reservoir ($40 \text{ }^\circ\text{C}$ and 80 bar, to ensure CO_2 at supercritical conditions – SC CO_2) for 1, 4, 16 and 64 days.

The brine used in the experiments is a natural brine from an old borehole from a saline aquifer (Torredonjimeno, Jaen, Spain)

with natural flow (2 l/s) on the surface; its conductivity at $20 \text{ }^\circ\text{C}$ is $162.014 \text{ } \mu\text{S/cm}$.

The experiment was conducted in a static Autoclave chamber (without CO_2 flow during the test). The tests began with the immersion of gabbro specimens (217 cm^3) in natural brine (600 cm^3) at the autoclave chamber, after which the CO_2 is injected. The final volume of CO_2 in chamber (at 80 bar and $40 \text{ }^\circ\text{C}$) was approximately 1183 cm^3 . In general, free-phase supercritical CO_2 (SC CO_2) was not in contact with the rock, as SC CO_2 migrates to the top of the test chamber due to density contrasts with the brine.

For the full characterization of rock specimens and co-existent brine, a multi-analytical approach was used:

- i. X-ray powder and in-situ diffractograms were produced using a Bruker AXS-D8 Advance (Bruker Corp, Billerica, Mass. USA) with Cu-K α radiation ($\lambda = 0.1540598 \text{ nm}$), under the following conditions: angular scanning between 3° and 75° (2θ), velocity scanning of $0.05^\circ 2\theta/\text{s}$, accelerating voltage of 40 kV, and current of 40 mA. The mineralogical composition of specimen surfaces was investigated by means of in-situ grazing incidence geometry experiments with incidence of 1° and 2θ scanning from 8 to 60° ;
- ii. surface sample analysis was performed with a Hitachi S-3700N SEM (Hitachi High Technologies, Berlin, Germany) coupled with a Bruker XFlash 5010 SDD detector (Bruker Corp, Billerica, Mass. USA), under low vacuum at 40 Pa and a current of 20 kV;
- iii. infrared spectra were obtained with a spectral resolution of 4 cm^{-1} (32 scans, in the $4000\text{--}650 \text{ cm}^{-1}$ of the selected area) with a Bruker Hyperion 3000 spectrometer equipped with a single point MCT detector cooled with liquid nitrogen and a $20\times$ ATR objective with a Ge crystal of $80 \text{ } \mu\text{m}$ diameter;
- iv. the chemical composition of the brine was determined at IGME Laboratories (Tres Cantos, Spain) by the combination of ion chromatography (Dionex 600 de Vertex), inductively coupled plasma optical emission spectrometry (ICP-OES) (ARIAN VISTA MPX), pH and conductivity measurements, both before and after the experiment;
- v. Iron brine content determination was performed at HERCULES Laboratory (Évora), with an Agilent 8800 ICP Triple Quad (ICP-QQQ), operating with a RF power of 1550 W, RF matching of 1.7 V, a sample depth of 10 mm, carrier gas (Ar) of 1.1 L/min and Plasma Gas (Ar) of 15 L/min. Prior to the analysis, the equipment was calibrated with a tune solution from Agilent and the sensitivity and resolution was optimized as well as the doubly charged ions ($< 1.84\%$) and oxides ($< 1.10\%$) were minimized.

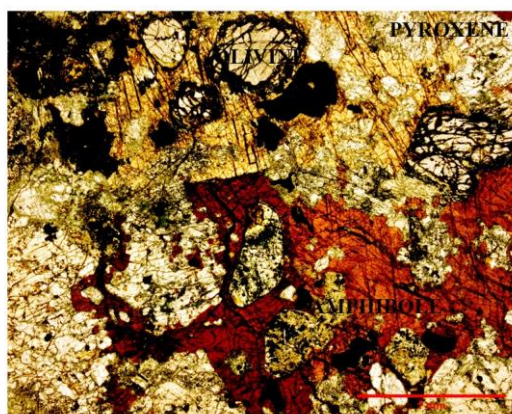
The analyses on specimens and brine were performed before and after the carbonation experiments, preserving the analytical conditions. In the case of analysis by destructive techniques (e.g. XRD powder) the comparison was made with the reference specimens (*i.e.* 0 days).

4. Results

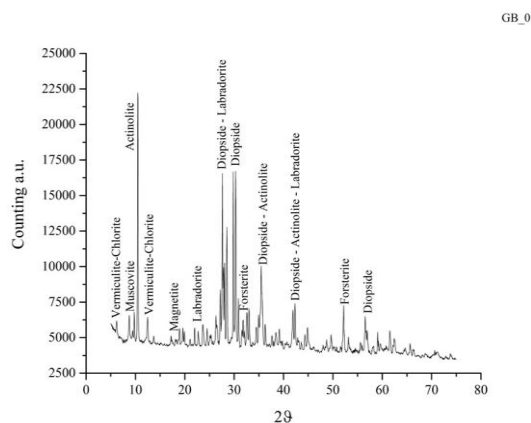
4.1. Gabbro

The gabbro displays a medium to coarse igneous texture that preserves the ferromagnesian mineral phases (olivine, pyroxene, amphibole and biotite), plagioclase and primary ilmenite (Fig. 2), although occasionally showing accessory alteration products (*e.g.* chlorite, actinolite).

After interaction of the rock specimens with the CO_2 saturated brine in the Autoclave chamber, an increase in dissolution of gabbro can be perceived (Fig. 3); after the 1-day



a



b

Figure 2. a) Microphotograph of gabbro under Polarized Light Microscope; b) difratogram of powdered gabbro (0 days).

Figura 2. a) Microfotografia de Gabro com Microscópio de Luz Polarizada; b) difratograma em amostra de gabro pulverizada (0 dias).

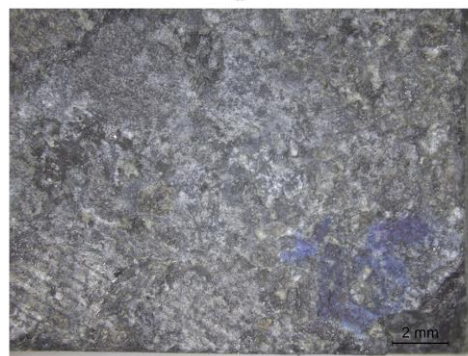
experiment there is a noticeable surface roughness, which increases for the longer time experiments and eventually leads to material fragmentation for the 16-day and 64-day experiments.

Petrographic analysis and powder-XRD on gabbro before and after contact with the brine shows no significant mineralogical differences besides salt precipitation. XRD on the surface of gabbro specimen (Fig. 4) after 64-day experiments reveals the presence of salts, halite and gypsum, and clay minerals.

The BSE images obtained before and after each experiment (Fig. 5a, b) essentially shows an increase of silicate dissolution, reflected in a higher surface roughness and highlighting of minerals cleavages. The new added phases display different reflectance and, according with EDS maps distribution (Fig. 5c), correspond to significant enrichment in chlorine (Cl), sodium (Na), sulphur (S) and carbon (C). The increase in Na, Cl, S and Calcium (Ca) is consistent with the presence of halite and gypsum detected by XRD at surface. However, the carbon observed at the surface is not related with the crystallization of carbonates. The ATR-FTIR spectra (Fig. 6a, b) of these carbon-



a



b

Figure 3. Stereozoom microscope images of specimen #15 before (a) and after 16 days (b) within brine at 40 °C and 80 bar.

Figura 3. Imagens de microscópio estereoscópico do provete #15: a) antes da salmoura; b) após de imersão em salmoura (40 °C e 80 bar) depois de 16 dias.

enriched areas present the characteristic infrared absorption bands of a cutting oil (Fig. 6b, red spectrum), namely: (i) the triglyceride pattern of the carbonyl stretching of the ester ($C=O$, 1736 cm^{-1}); (ii) the infrared profile bands related to the C-H absorptions from the fatty acid chain due to the methylene stretching at circa 2918 cm^{-1} and 2851 cm^{-1} ($\nu_{\text{asym}}(\text{CH}_2)$ and $\nu_{\text{sym}}(\text{CH}_2)$, respectively); and (iii) the methyl stretching at 2955 cm^{-1} and 2874 cm^{-1} ($\nu_{\text{asym}}(\text{CH}_3)$ and $\nu_{\text{sym}}(\text{CH}_3)$, respectively). Despite these infrared fingerprints pointing to the presence of tryglicerides-enriched areas, its origin is still to be clarified. Also, the analysis by ATR-FTIR of this sample (gabbro after 16-days of interaction with CO_2) revealed the decrease of intensity of the absorption band related to the silicate groups at 1054 cm^{-1} present in the original sample (Fig. 6a, black spectrum), and the absence (or residual presence) of carbonation, evidenced by the absence of the absorption band at circa 1420 cm^{-1} related to the $\nu(\text{CO}_3^{2-})$ (Fig. 6b, red spectrum).

4.2 Brine

As for the high salinity brine, pH varied during the experiments from 6.85 (brine without CO_2) to 4.5, 4.87, 5.1 and 5.5, for the 1, 4, 16 and 64-day for the brine and CO_2 mixture, respectively (Tab. 1).

In general, the behaviour of cations in solution is variable, notwithstanding the tendency for Na^+ and Ca^{2+} decreasing

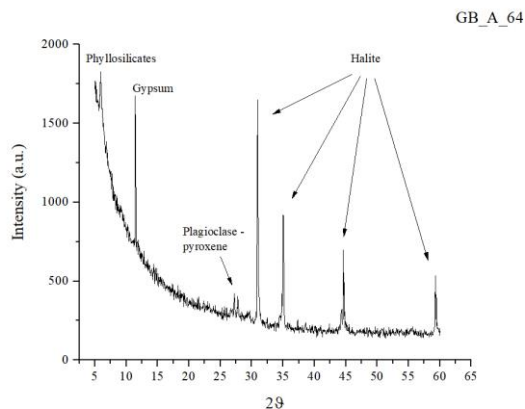


Figure 4. Diffractogram obtained on the surface of gabbro after 64 days within brine and CO₂.

Figura 4. Difractograma obtido na superfície do gabro após 64 dias imerso em salmoura com CO₂.

concentrations, whereas those of K⁺, Mg²⁺ and total-Fe increase. The relative abundances of Cl⁻, SO₄²⁻ and SiO₂ have a more unpredictable behaviour, displaying either enrichment or impoverishment trends along the four experiments.

5. Discussion

Most of the projects developed on *in situ* carbonation deals with ultrabasic or basic volcanic rocks. The reason lies on the availability of cations present in mafic compositions such as Mg²⁺, Fe²⁺ and Ca²⁺ than can link to dissolved CO₂ and crystallize as carbonates (*e.g.* magnesite, siderite or calcite). In the InCarbon project, rocks with similar mineralogy were tested aiming to, in a first analysis, verify the behaviour of cations released from a coarser texture, after immersion in brines injected with SC CO₂.

In general, the parameters affecting the rate of carbonate-forming are brine composition, temperature, pressure and pH (Soong *et al.*, 2006). Although the natural brine has a near neutral pH, the acidity will increase once CO₂ is added (*e.g.* Liu and Maroto-Valer, 2010).

Considering the 4 experiments, the development of any carbonate phase was not observed or detected by means of SEM-EDS, XRD or FTIR. Since pH values remained low in all experiments, the environmental acidity might have inhibited the formation of siderite, the most expectable carbonate phase to precipitate (Gysi and Stefánsson, 2012). Although some modelling studies suggest the possibility of siderite formation at pH < 5 (Snæbjörnsdóttir *et al.*, 2018) or calcite and magnesite at pH ~ 5 (McGrail *et al.*, 2006), our experiments were not successful in detecting such phases. In addition, it was not possible to perceive magnesite nucleation, despite of olivine dissolution, as reported in other works running under similar experimental conditions (Giammar *et al.* 2005). In this regard, supplementary investigations reveal that the growth of Ca-Mg-Fe carbonates occurs at pH < 6.5, whereas the formation of Ca-Mg carbonates took place only at pH > 6.5 (Gysi and Stefánsson, 2012). Moreover, the fact that saturation values of different carbonates and brine equilibrium have not been reached or the possible undetected micro-nucleation, are hypotheses that cannot be ruled out.

In the present work, the variability of cation concentrations in the brine reflects the reaction dynamics imposed by the

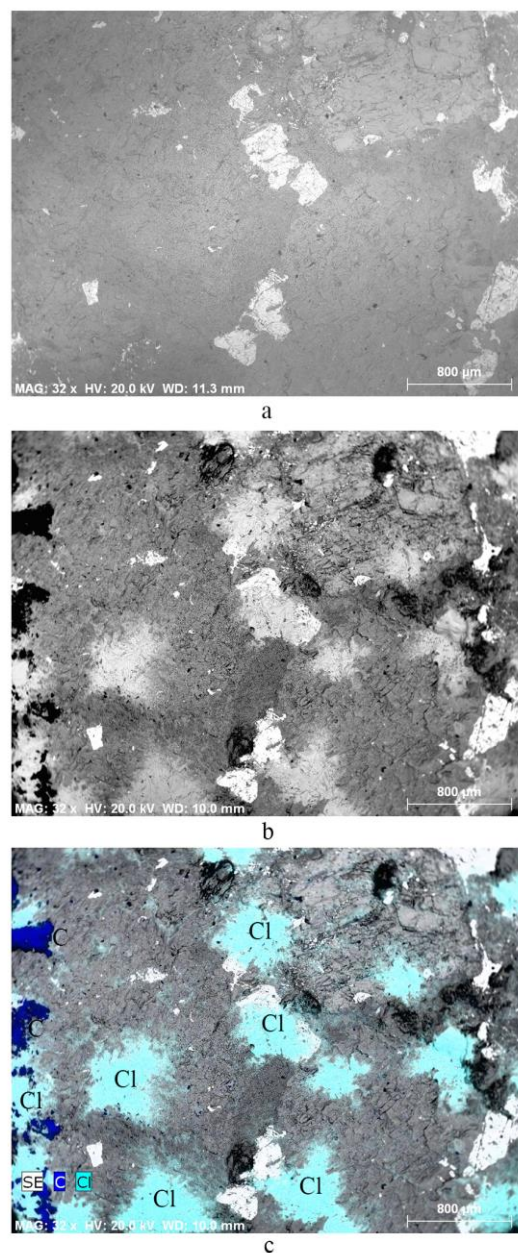


Figure 5. VP-SEM-EDS results comparison of samples before (a) and after (b, c) 16 days immersed in brine. C – carbon; Cl – chlorine; BSE – backscattered electrons.

Figura 5. resultados de VP-MEV-EDX dos provetes antes (a) e após (b, c) imersão em salmoura com CO₂ durante 16 dias. C – carbon; Cl – cloro; BSE – eletrões retro-difundidos.

composition of the high salinity brine, silicates dissolution and crystallization of halite and gypsum. While the measured concentrations of SiO₂, Fe and K at the end of the 4 experiments are consistent with the continuous dissolution of silicates, the behaviour of Na⁺, Ca²⁺ is more difficult to interpret given the relationship with both dissolution of silicates and crystallization of salts at the gabbro surface. The HCO₃⁻ does not present significant changes due to CO₂ loss (depressurization) when the test is completed and the chamber is open. As well, measurement of pH values is conditioned by the release of CO₂ during depressurization after chamber opening, and thus the acidity during the experiments should be even lower than those measured when the chamber is decompressed (< 5.5).

Table 1. Brine characterization. Chemical analysis of pure brine and brine taken from the reaction chambers. Uncertainty (Na⁺: 14%; K⁺: 12%, Ca²⁺: 10%, Mg²⁺: 20%, Cl⁻: 12%; SO₄²⁻: 14%; HCO₃⁻: 10%; NO₃⁻: 14%; SiO₂: 10%; pH: 0.2; Conductivity: 10%) and detection limit (Na⁺: 2mg; K⁺: 1mg; Ca⁺: 1mg; Mg⁺: 1mg; Cl⁻: 1 mg; SO₄²⁻: 1 mg; HCO₃⁻: 1 mg; NO₃⁻: 0.5 mg; SiO₂: 1mg; Conductivity: 100 μs/cm) given by IGME Laboratory. Iron quantification was done by ICP-MS. Precision of the analysis 2-5%, LOD (Limit of detection) – 7.5 ppb, LOQ (Limit of Quantification) – 75 ppb, BEC (background-equivalent concentration) – 250.9 ppb.

Tabela 1. Caracterização da salmoura. Análise química da salmoura pura e da salmoura retirada das câmaras de reação. Incerteza (Na⁺: 14%; K⁺: 12%, Ca²⁺: 10%, Mg²⁺: 20%, Cl⁻: 12%; SO₄²⁻: 14%; HCO₃⁻: 10%; NO₃⁻: 14%; SiO₂: 10%; pH: 0,2; Condutividade: 10%) e limite de deteção (Na⁺: 2mg; K⁺: 1mg; Ca⁺: 1mg; Mg⁺: 1 mg; Cl⁻: 1 mg; SO₄²⁻: 1 mg; HCO₃⁻: 1 mg; NO₃⁻: 0,5 mg; SiO₂: 1mg; Condutividade: 100 μs / cm) fornecida pelo laboratório IGME. A quantificação do ferro foi obtida através de ICP-MS. Precisão da análise 2-5%. LOD (Limite de deteção) – 7,5 ppb, LOQ (Limite de Quantificação) – 75 ppb, BEC (concentração equivalente a fundo) – 250,9 ppb.

days→	Brine before CO ₂		Brine after CO ₂ experiments		
	0	1	4	16	64
Na ⁺ (ppm)	85450	67105	86015	84050	79680
K ⁺ (ppm)	260	260	305	310	415
Ca ²⁺ (ppm)	2050	1900	1890	1860	1650
Mg ²⁺ (ppm)	630	660	680	730	630
Fe (ppm)	5.16	6.02	11.25	18.88	26.37
Cl ⁻ (ppm)	133500	104000	133000	124000	119000
SO ₄ ²⁻ (ppm)	5400	5400	5600	5700	5300
HCO ₃ ⁻ (ppm)	40	35	38	35	33
NO ₃ ⁻ (ppm)	0	0	0	0	0
SiO ₂ (ppm)	11.5	20	24.9	39	37
pH	7.05	5.66	6.38	6.38	5.84
Conductivity (μs/cm)	80000	85000	80000	75000	75000

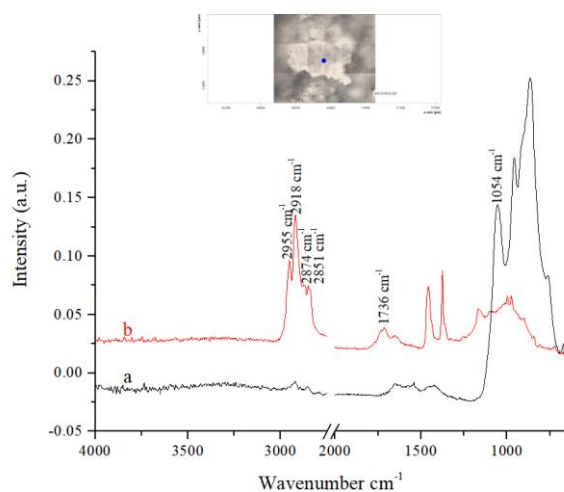


Figure 6. ATR-FTIR spectra of carbon-enriched areas (a - black) and of a standard spectrum of a cutting oil (b - red spectrum). The inset shows the spot of analysis on specimen after 16-day experiment.

Figura 6. Espectro ATR-FTIR de zonas enriquecidas em carbono (a - preto) comparativamente a um espectro de óleo de corte (b - vermelho). A imagem mostra o ponto de análise após o ensaio de 16 dias.

Nevertheless, the increase in pH correlates positively with the time of rock/brine interaction. In order to accelerate the pH

increase, future experiments will consider the effect triggered by the rising of rock / CO₂ saturated brine ratio.

6. Final remarks

After interaction of gabbro and brine saturated with CO₂ for 1, 4, 16 or 64 days, no carbonate formation was detected. However, an intensification of silicates dissolution was noticeable, resulting in an increased roughness of the surface of specimens. This mechanism of dissolution is in agreement with the increase of silica and iron concentration in solution. Nevertheless, the behaviour of cations in the brine after experiment is complex and needs to be better understood. The results obtained should be complemented with analyses of elementary geochemistry and TGA on gabbro specimens. Future experiments will evaluate the relevance of the rock/brine/CO₂ relative proportions.

Acknowledgments

Authors gratefully acknowledge the FCT support through the Projct InCarbon - Carbonatação in-situ para redução de emissões de CO₂ de fontes energéticas e industriais no Alentejo (PTDC/CTA- GEO/31853/2017). The authors would like to thank the reviewers António Mateus and Pedro Ferreira for their contribution to the improvement of the article.

References

- Andreani, M., Luquot, L., Gouze, P., Godard, M., Hoisé, E., Gibert, B., 2009. Experimental Study of Carbon Sequestration Reactions Controlled by the Percolation of CO₂-Rich Brine through Peridotites. *Environ. Sci. Technol.*, **43**(4): 1226-1231. DOI:10.1021/es8018429.
- Bachu, S., 2000. Sequestration of CO₂ in geological media: Criteria and approach for site selection in response to climate change. *Energy Convers. Manag.*, **41**: 953-970. DOI:10.1016/S0196-8904(99)00149-1.
- Benson, S. M., Cole, D. R., 2008. CO₂ sequestration in deep sedimentary formations. *Elements*, **4**: 325-331. DOI: 10.2113/gselements.4.5.325.
- Canilho, M. H., 1972. Estudo geológico-petrográfico do maciço eruptivo de Sines. *Bol. Mus. Lab. Min. FCUL*, **12**: 77-161.
- Canilho, M. H., Abranches, M. C., 1982. Rb-Sr geochronology of the Sines alkaline complex. *Comun. Serv. Geol. Port.*, **68**: 237-240.
- Carvalho, J. P. G., Torres, L. M., Afilhado, A., 1998. Delimitação do maciço sub-vulcânico de Sines offshore a partir de dados geofísicos. *Comun. Serv. Geol. Port.*, **84**: D57-D60.
- Druckemiller, M. L., Maroto-Valer, M. M., 2005. Carbon sequestration using brine of adjusted pH to form mineral carbonates. *Fuel Processing Technology*, **86**(14-15): 1599-1614. DOI: 10.1016/j.fuproc.2005.01.007.
- Ferreira, M. R. P., Macedo, C. R., 1979. K-Ar ages of the Permian-Mesozoic basaltic activity in Portugal. Abstracts VI, In: *Europ. Col. Geochron., Cosmochron. and Isotope Geology*, Norway, 26-27.
- Gaus, I., 2010. Role and impact of CO₂-rock interactions during CO₂ storage in sedimentary rocks. *Int. J. Greenh. Gas Control*, **4**: 73-89.
- Giammar, D. E., Bruant, R. G., Peters, C. A., 2005. Forsterite dissolution and magnesite precipitation at conditions relevant for deep saline aquifer storage and sequestration of carbon dioxide. *Chem. Geol.*, **217**: 257-276. DOI: 10.1016/j.chemgeo.2004.12.013.
- Gysi, A., Stefánsson, A., 2012. Mineralogical aspects of CO₂ sequestration during hydrothermal basalt alteration - An experiment study at 75 to 250 °C and elevated pCO₂. *Chem. Geol.*, **306-307**: 146-159. DOI: 10.1016/j.chemgeo.2012.03.006.
- Inverno, C., Manuppella, G., Zbyszewski, G., Pais, J., Ribeiro, L., 1993. *Notícia Explicativa da Folha 42-C Santiago do Cacém da Carta Geológica de Portugal na escala 1/50 000*. Serviços Geológicos de Portugal, 75.
- Izgec, O., Demiral, B., Bertin, H. J., Akin, S., 2008. CO₂ injection into saline carbonate aquifer formations I: Laboratory investigation. *Transp. Porous Media*, **72**: 1-24.
- Kaszuba, J. P., Janecky, D. R., Snow, M. G., 2005. Experimental evaluation of mixed fluid reactions between supercritical carbon

- dioxide and NaCl brine: Relevance to the integrity of a geologic carbon repository. *Chem. Geol.*, **217**: 277-293. DOI: 10.1016/j.chemgeo.2004.12.014.
- Ketzer, J. M., Iglesias, R., Einloft, S., Dullius, J., Ligabue, R., De Lima, V., 2009. Water-rock-CO₂ interactions in saline aquifers aimed for carbon dioxide storage: experimental and numerical modeling studies of the Rio Bonito Formation (Permian), southern Brazil. *Appl. Geochem.*, **24**: 760-767. DOI: 10.1016/j.apgeochem.2009.01.001.
- Klein, F., McCollom, T. M., 2013. From serpentinization to carbonation: New insights from a CO₂ injection experiment. *Earth and Planetary Science Letters*, **379**: 137-145. DOI: 10.1016/j.epsl.2013.08.017.
- Liu, Q., Maroto-Valer, M. M., 2010. Investigation of the pH effect of a typical host rock and buffer solution on CO₂ sequestration in synthetic brines. *Fuel Processing Technology*, **91**: 1321-1329. DOI: 10.1016/j.fuproc.2010.05.002.
- Mateos-Redondo, F., Kovacs, T., Berrezueta, E., 2018. Petrographic and Petrophysical Characterization of Detrital Reservoir Rocks for CO₂ Geological Storage (Utrillas and Escucha Sandstones, Northern Spain). *Geosciences*, **8**: 246. DOI: 10.3390/geosciences8070246.
- McGrail, B. P., Schaef, H. T., Ho, A. M., Chien, Y. J., Dooley, J. J., Davidson, C. L., 2006. Potential for carbon dioxide sequestration in flood basalts. *J. Geophys. Res.*, **111**, B12201, 13. DOI: 10.1029/2005JB004169.
- McGrail, B. P., Spane, F. A., Amonette, J. E., Thompson, C. R., Brown, C. F., 2014. Injection and monitoring at the Wallula basalt pilot project. *Energy Procedia*, **63**: 2939-2948. DOI: 10.1016/j.egypro.2014.11.316.
- Miranda, R., Valadares, V., Terrinha, P., Mata, J., Azevedo, M. R., Gaspar, M., Kullberg, J. C., Ribeiro, C., 2009. Age constraints on the Late Cretaceous alkaline magmatism on the West Iberian margin. *Cretaceous Res.*, **30**: 575-586. DOI: j.cretres.2008.11.002.
- Ribeiro, A., Antunes, M. T., Ferreira, M. P., Rocha, R. B., Soares, A. F., Zbyszewski, G., Moitinho de Almeida, F., De Carvalho, D., Monteiro, J. H., 1979. *Introduction à la géologie générale du Portugal*. Serviços Geológicos de Portugal, Lisboa, 114.
- RCN20150, 2019. *Decarbonizing is not an empty word it is a call to action*. Available in <https://descarbonizar2050.pt/en/>. Access in 28/10/2019.
- Saeedi, A., Rezaee, R., Evans, B., Clennell, B., 2011. Multiphase flow behaviour during CO₂ geo-sequestration: Emphasis on the effect of cyclic CO₂-brine flooding. *J. Petrol. Sci. Eng.*, **79**: 65-85. DOI: 10.1016/j.petrol.2011.07.007.
- Sayegh, S. G., Krause, F. F., Girard, M., DeBree, C., 1990. Rock/fluid interactions of carbonated brines in a sandstone reservoir: Pembina Cardium, Alberta, Canada. *SPE Formation Evaluation*, **5**: 399-405. DOI: 10.2118/19392-PA.
- Snæbjörnsdóttir, S. O., Gislason, S. R., Galeczka, I. M., Oelkers, E. H., 2018. Reaction path modelling of in-situ mineralisation of CO₂ at the CarbFix site at Hellisheidi, SW-Iceland. *Geochim. Cosmochim. Ac.*, **220**: 348-366. DOI: 10.1016/j.gca.2017.09.053.
- Soong, Y., Fauth, D. L., Howard, B. H., Jones, J. R., Harrison, D. K., Goodman, A. L., Gray, M. L., Frommel, E. A., 2006. CO₂ sequestration with brine solution and fly ashes. *Energy Conversion and Management*, **47**(13-14): 1676-1685. DOI: 10.1016/j.enconman.2005.10.021.
- Teixeira, C., 1962. La structure annulaire subvolcanique des massifs éruptifs de Sintra, Sines et Monchique. *Est. Cient. of. Prof. Carrington da Costa*, J. I. U., Lisboa, 461-49.